

Interleave-Division Multiple-Access¹

*Li Ping, Lihai Liu, K. Y. Wu, and W. K. Leung, email: eeliping@cityu.edu.hk
Department of Electronic Engineering, City University of Hong Kong*

Abstract – This paper provides a comprehensive study of interleave-division multiple-access (IDMA) systems. The IDMA receiver principles for different modulation and channel conditions are outlined. A semi-analytical technique is developed based on the density evolution technique to estimate the bit-error-rate (BER) of the system. It provides a fast and relatively accurate method to predict the performance of the IDMA scheme. Simulation examples are provided to demonstrate the advantages of the IDMA scheme in terms of both bandwidth and power efficiencies. For example, with simple convolutional/repetition codes, overall throughputs of 3 bits/chip with one receive antenna and 6 bits/chip with two receive antennas are observed for systems with as many as about 100 users.

Keywords – CDMA, channel capacity, iterative decoding, multi-user detection.

I. INTRODUCTION

The performance of code-division multiple-access (CDMA) systems is mainly limited by multiple access interference (MAI) and intersymbol interference (ISI). In the wake of the success of turbo codes [1], turbo-type iterative multi-user detection (MUD) has been extensively studied [2]-[10] to mitigate MAI and ISI, and significant progress has been made.

A conventional random waveform CDMA (RW-CDMA) system (such as IS-95) involves separate coding and spreading operations. Theoretical analysis [11][12] shows that the optimal multiple access channel (MAC) capacity is achievable when the entire bandwidth expansion is devoted to coding. This suggests combining coding and spreading using low-rate codes to maximize coding gain [11][13]. In this case, interleavers can be employed to distinguish signals from different users. The principle has been studied previously and its potential advantages have been demonstrated [2][14]-[20]. Ref. [2] showed the possibility of employing interleaving for

¹ This work was fully supported by a grant from the Research Grant Council of the Hong Kong Special Administrative Region, China [Project No. CityU 1164/03E]. The material in this paper was presented in part at the IEEE Vehicular Technology Conference 2003 and IEEE Wireless Communications and Networking Conference 2003.

user separation in coded systems. Ref. [14] proposed narrow-band coded-modulation schemes in which trellis code structures are used for user separation and interleaving is considered as an option. For wideband systems, the performance improvement by assigning different interleavers to different users in conventional CDMA has been demonstrated in [15] and [16]. Ref. [17] studied a chip interleaved CDMA scheme and a maximal-ratio-combining (MRC) technique for MACs with ISI. It clearly demonstrated the advantages of introducing chip-level interleavers. An interleaver-based multiple access scheme has also been studied in [18]-[20] for high spectral efficiency, improved performance and low receiver complexity. This scheme relies on interleaving as the only means to distinguish the signals from different users, and hence it has been called interleave-division multiple-access (IDMA). IDMA inherits many advantages from CDMA, in particular, diversity against fading and mitigation of the worst-case other-cell user interference problem. Furthermore, it allows a very simple chip-by-chip iterative MUD strategy [20]. The normalized MUD cost (per user) is independent of the number of users.

In this paper, we will provide a comprehensive study of the IDMA scheme, incorporating the principles developed in [18][20]. We will present several low-cost detection algorithms for different channel conditions, namely, real-single-path, real-multi-path and complex-multi-path channels. These algorithms are very simple and efficient, as confirmed by simulation results. We will also develop a semi-analytical technique based on the density evolution technique [9], [21]-[23] to estimate the bit-error rate (BER) performance of these algorithms. This represents a fast and accurate method to predict the performance of the IDMA scheme. Both semi-analytical and simulation results are provided to demonstrate the advantages of the IDMA scheme. For example, with simple convolutional/repetition codes, overall throughputs of 3 bits/chip with one receive antenna and 6 bits/chip with two receive antennas are observed for systems with as many as about 100 users. More sophisticated low-rate codes can also be used for further performance enhancement, as illustrated by comparison between low-rate and high-rate coded IDMA systems.

II. IDMA TRANSMITTER AND RECEIVER PRINCIPLES

A. IDMA Transmitter and Receiver Structures

The upper part of Fig. 1 shows the transmitter structure of the multiple access scheme under consideration with K simultaneous users. The input data sequence \mathbf{d}_k of user- k is encoded based on a low-rate code C , generating a coded sequence $\mathbf{c}_k \equiv [c_k(1), \dots, c_k(j), \dots, c_k(J)]^T$, where J is the frame length. The elements in \mathbf{c}_k are referred to as coded bits. Then \mathbf{c}_k is permuted by an interleaver π_k , producing $\mathbf{x}_k \equiv [x_k(1), \dots, x_k(j), \dots, x_k(J)]^T$. Following the CDMA convention, we call the elements in \mathbf{x}_k “chips”. Users are solely distinguished by their interleavers, hence the name interleave-division multiple-access (IDMA).

The key principle of IDMA is that the interleavers $\{\pi_k\}$ should be different for different users. We assume that the interleavers are generated independently and randomly. These interleavers disperse the coded sequences so that the adjacent chips are approximately uncorrelated, which facilitates the simple chip-by-chip detection scheme discussed below.

We adopt an iterative sub-optimal receiver structure, as illustrated in Fig. 1, which consists of an elementary signal estimator (ESE) and K single-user *a posteriori* probability (APP) decoders (DECs). The multiple access and coding constraints are considered separately in the ESE and DECs. The outputs of the ESE and DECs are extrinsic log-likelihood ratios (LLRs) about $\{x_k(j)\}$ defined below [18]-[20]:

$$e(x_k(j)) \equiv \log \left(\frac{\Pr(x_k(j) = +1)}{\Pr(x_k(j) = -1)} \right), \quad \forall k, j. \quad (1)$$

These LLRs are further distinguished by subscripts, i.e., $e_{ESE}(x_k(j))$ and $e_{DEC}(x_k(j))$, depending on whether they are generated by the ESE or DECs. A global turbo-type iterative process is then applied to process the LLRs generated by the ESE and DECs [1][18], as detailed below.

B. The Basic ESE Function

We first assume that the channel has no memory. After chip-matched filtering, the received signal from K users can be written as

$$r(j) = \sum_{k=1}^K h_k x_k(j) + n(j), \quad j = 1, 2, \dots, J \quad (2)$$

where h_k is the channel coefficient for user- k and $\{n(j)\}$ are samples of an AWGN process with variance $\sigma^2 = N_0/2$. We assume that the channel coefficients $\{h_k\}$ are known *a priori* at the

receiver. Due to the use of random interleavers $\{\pi_k\}$, the ESE operation can be carried out in a chip-by-chip manner, with only one sample $r(j)$ used at a time. Rewrite (2) as

$$r(j) = h_k x_k(j) + \zeta_k(j) \quad (3a)$$

where

$$\zeta_k(j) \equiv r(j) - h_k x_k(j) = \sum_{k' \neq k} h_{k'} x_{k'}(j) + n(j) \quad (3b)$$

is the distortion (including interference-plus-noise) in $r(j)$ with respect to user- k . From the central limit theorem, $\zeta_k(j)$ can be approximated as a Gaussian variable, and $r(j)$ can be characterized by a conditional Gaussian probability density function

$$p(r(j) | x_k(j) = \pm 1) = \frac{1}{\sqrt{2\pi \text{Var}(\zeta_k(j))}} \exp\left(-\frac{(r(j) - (\pm h_k + \text{E}(\zeta_k(j))))^2}{2\text{Var}(\zeta_k(j))}\right) \quad (4)$$

where $\text{E}(\cdot)$ and $\text{Var}(\cdot)$ are the mean and variance functions, respectively.

The following is a list of the ESE detection algorithm based on (2)~(4) [18], assuming that the *a priori* statistics $\{\text{E}(x_k(j))\}$ and $\{\text{Var}(x_k(j))\}$ are available (see Section II.F).

Algorithm 1. Chip-by-Chip Detection in a Single-Path Channel

Step (i): Estimation of Interference Mean and Variance

$$\text{E}(r(j)) = \sum_k h_k \text{E}(x_k(j)), \quad (5a)$$

$$\text{Var}(r(j)) = \sum_k |h_k|^2 \text{Var}(x_k(j)) + \sigma^2, \quad (5b)$$

$$\text{E}(\zeta_k(j)) = \text{E}(r(j)) - h_k \text{E}(x_k(j)), \quad (5c)$$

$$\text{Var}(\zeta_k(j)) = \text{Var}(r(j)) - |h_k|^2 \text{Var}(x_k(j)). \quad (5d)$$

Step (ii): LLR Generation

$$e_{ESE}(x_k(j)) = 2h_k \cdot \frac{r(j) - \text{E}(\zeta_k(j))}{\text{Var}(\zeta_k(j))}. \quad (6)$$

Comments:

- Assuming independent $\{x_k(j)\}$, (5) is a straightforward consequence of (2) and (3b).
- Step (ii) is obtained by evaluating (1) based on (4).
- Algorithm 1 is an extremely simplified form of that derived in [4] when the spreading sequences are all of length-1.
- The cost in (5a) and (5b), i.e., generating $\text{E}(r(j))$ and $\text{Var}(r(j))$, are shared by all users, costing only three multiplications and two additions per coded bit per user. Overall, the ESE

operations in (5)~(6) cost only seven multiplications and five additions per coded bit per user, which is very modest. Interestingly, the cost per information bit per user is independent of the number of users K . This is considerably lower than that of other alternatives. For example, the well-known MMSE algorithm in [4] has complexity of $O(K^2)$.

C. The ESE Function for Multi-Path Channels

We now consider the ESE function in a quasi-static multi-path fading channel with memory length $L-1$. Let $\{h_{k,0}, \dots, h_{k,L-1}\}$ be the fading coefficients related to user- k . After chip-matched filtering, the received signal can be represented by

$$r(j) = \sum_{k=1}^K \sum_{l=0}^{L-1} h_{k,l} x_k(j-l) + n(j), \quad j = 1, \dots, J + L - 1. \quad (7)$$

We write

$$r(j+l) = h_{k,l} x_k(j) + \zeta_{k,l}(j) \quad (8a)$$

where

$$\zeta_{k,l}(j) = r(j+l) - h_{k,l} x_k(j). \quad (8b)$$

The similarity between (8a) and (3a) is clearly seen. Assume again BPSK signaling and real channel coefficients. Algorithm 2 below is a straightforward extension of Algorithm 1.

Algorithm 2. Chip-by-Chip Detection in a Multi-Path Channel

Step (i): Estimation of Interference Mean and Variance

$$\mathbb{E}(r(j)) = \sum_{k,l} h_{k,l} \mathbb{E}(x_k(j-l)), \quad (9a)$$

$$\text{Var}(r(j)) = \sum_{k,l} |h_{k,l}|^2 \text{Var}(x_k(j-l)) + \sigma^2, \quad (9b)$$

$$\mathbb{E}(\zeta_{k,l}(j)) = \mathbb{E}(r(j+l)) - h_{k,l} \mathbb{E}(x_k(j)), \quad (9c)$$

$$\text{Var}(\zeta_{k,l}(j)) = \text{Var}(r(j+l)) - |h_{k,l}|^2 \text{Var}(x_k(j)). \quad (9d)$$

Step (ii): LLR Generation and Combining

$$e_{ESE}(x_k(j))_l = 2h_{k,l} \cdot \frac{r(j+l) - \mathbb{E}(\zeta_{k,l}(j))}{\text{Var}(\zeta_{k,l}(j))}, \quad (10a)$$

$$e_{ESE}(x_k(j)) = \sum_{l=0}^{L-1} e_{ESE}(x_k(j))_l. \quad (10b)$$

Comments:

- It is easy to see the connection between (9) and (5).

- From (7), each $x_k(j)$ is observed on L successive samples $\{r(j), r(j+1), \dots, r(j+L-1)\}$. Assume that the distortion terms with respect to $x_k(j)$ in these L samples, i.e., $\{\zeta_{k,0}(j), \zeta_{k,1}(j), \dots, \zeta_{k,L-1}(j)\}$, are un-correlated. Then the overall *a posteriori* probabilities for $x_k(j) = \pm 1$ are the products of the individual *a posteriori* probabilities generated from $\{r(j), r(j+1), \dots, r(j+L-1)\}$. Hence the LLRs for $x_k(j)$ can be directly summed as in (10b). This LLR combining (LLRC) technique is similar to the rake operation used in CDMA.
- The overall complexity is approximately L times of that of Algorithm 1.

The un-correlation assumption mentioned above is only approximate, but it greatly simplifies the matter. The complexity (per coded bit per user) for Algorithm 2 is $O(L)$. There are other alternative treatments for channels with memory. One is the joint Gaussian (JG) technique [19] that takes into consideration the correlation among $\{\zeta_{k,0}(j), \zeta_{k,1}(j), \dots, \zeta_{k,L-1}(j)\}$. This technique leads to improved performance but also increased cost ($O(L^2)$). Another alternative is the maximum ratio combining (MRC) technique [17], in which $\mathbf{r} \equiv \{r_j\}$ is passed through K MRC filters, each matched to the L tap-coefficients for a particular user. An MMSE detection is then applied to generate $\{e_{ESE}(x_k(j))\}$. The related complexity is $O(KL)$ [17].

Generally speaking, the JG technique demonstrates better performance but this becomes noticeable only when the number of users is very large or when the rate of C is high. Overall, the LLRC method is a good compromise between complexity and performance. See [19] for a detailed discussion.

D. The ESE Function for More Complex Channels

We now extend our discussion to more complex situations. We will use either superscripts “Re,” and “Im,” or function notations $\text{Re}(\cdot)$ and $\text{Im}(\cdot)$ to indicate real and imaginary parts, respectively. Consider quadrature-phase-shift-keying (QPSK) signaling,

$$x_k(j) = x_k^{\text{Re}}(j) + ix_k^{\text{Im}}(j), \quad (11)$$

where $i = \sqrt{-1}$, $x_k^{\text{Re}}(j)$ and $x_k^{\text{Im}}(j)$ are two coded bits from \mathbf{c}_k . For convenience, we still call the elements in \mathbf{x}_k “chips”. Note that in this case, each chip contains two coded bits. We adopt channel model (7) and expand it using complex channel coefficients $\{h_{k,l} = h_{k,l}^{\text{Re}} + ih_{k,l}^{\text{Im}}\}$ as

$$r(j) = \sum_{k,l} \left(h_{k,l}^{\text{Re}} x_k^{\text{Re}}(j-l) - h_{k,l}^{\text{Im}} x_k^{\text{Im}}(j-l) \right) + i \sum_{k,l} \left(h_{k,l}^{\text{Re}} x_k^{\text{Im}}(j-l) + h_{k,l}^{\text{Im}} x_k^{\text{Re}}(j-l) \right) + n(j) \quad (12)$$

where $\{n(j)\}$ are samples of a complex AWGN process with variance σ^2 per dimension. Denote by $\overline{h_{k,l}}$ the conjugate of $h_{k,l}$. Recall (8): $r(j+l) = h_{k,l} x_k(j) + \zeta_{k,l}(j)$. The phase shift due to $h_{k,l}$ is cancelled out in $\overline{h_{k,l}} r(j+l)$, which means that $\text{Im}(\overline{h_{k,l}} r(j+l))$ is not a function of $x_k^{\text{Re}}(j)$.

Therefore the detection of $x_k^{\text{Re}}(j)$ only requires

$$\text{Re}(\overline{h_{k,l}} r(j+l)) = |h_{k,l}|^2 x_k^{\text{Re}}(j) + \text{Re}(\overline{h_{k,l}} \zeta_{k,l}(j)). \quad (13)$$

Algorithm 3 below outlines the procedure to estimate $x_k^{\text{Re}}(j)$ based on (13).

Algorithm 3. Chip-by-Chip Detection in a Complex Multi-Path Channel

Step (i): Estimation of Interference Mean and Variance

$$\text{E}(r^{\text{Re}}(j)) = \sum_{k,l} \left(h_{k,l}^{\text{Re}} \text{E}(x_k^{\text{Re}}(j-l)) - h_{k,l}^{\text{Im}} \text{E}(x_k^{\text{Im}}(j-l)) \right), \quad (14a)$$

$$\text{E}(r^{\text{Im}}(j)) = \sum_{k,l} \left(h_{k,l}^{\text{Re}} \text{E}(x_k^{\text{Im}}(j-l)) + h_{k,l}^{\text{Im}} \text{E}(x_k^{\text{Re}}(j-l)) \right), \quad (14b)$$

$$\text{Var}(r^{\text{Re}}(j)) = \sum_{k,l} \left((h_{k,l}^{\text{Re}})^2 \text{Var}(x_k^{\text{Re}}(j-l)) + (h_{k,l}^{\text{Im}})^2 \text{Var}(x_k^{\text{Im}}(j-l)) \right) + \sigma^2, \quad (14c)$$

$$\text{Var}(r^{\text{Im}}(j)) = \sum_{k,l} \left((h_{k,l}^{\text{Im}})^2 \text{Var}(x_k^{\text{Re}}(j-l)) + (h_{k,l}^{\text{Re}})^2 \text{Var}(x_k^{\text{Im}}(j-l)) \right) + \sigma^2, \quad (14d)$$

$$\Psi(j) = \sum_{k,l} h_{k,l}^{\text{Re}} h_{k,l}^{\text{Im}} \left(\text{Var}(x_k^{\text{Re}}(j-l)) - \text{Var}(x_k^{\text{Im}}(j-l)) \right), \quad (15)$$

$$\text{E}\left(\text{Re}(\overline{h_{k,l}} \zeta_{k,l}(j))\right) = h_{k,l}^{\text{Re}} \text{E}(r^{\text{Re}}(j+l)) + h_{k,l}^{\text{Im}} \text{E}(r^{\text{Im}}(j+l)) - |h_{k,l}|^2 \text{E}(x_k^{\text{Re}}(j)), \quad (16a)$$

$$\begin{aligned} \text{Var}\left(\text{Re}(\overline{h_{k,l}} \zeta_{k,l}(j))\right) &= (h_{k,l}^{\text{Re}})^2 \text{Var}(r^{\text{Re}}(j+l)) + (h_{k,l}^{\text{Im}})^2 \text{Var}(r^{\text{Im}}(j+l)) \\ &\quad + 2h_{k,l}^{\text{Re}} h_{k,l}^{\text{Im}} \Psi(j+l) - |h_{k,l}|^4 \text{Var}(x_k^{\text{Re}}(j)). \end{aligned} \quad (16b)$$

Step (ii): LLR Generation and Combining

$$e_{ESE}(x_k^{\text{Re}}(j))_l = 2|h_{k,l}|^2 \cdot \frac{\text{Re}(\overline{h_{k,l}} r(j+l)) - \text{E}\left(\text{Re}(\overline{h_{k,l}} \zeta_{k,l}(j))\right)}{\text{Var}\left(\text{Re}(\overline{h_{k,l}} \zeta_{k,l}(j))\right)}, \quad (17a)$$

$$e_{ESE}(x_k^{\text{Re}}(j)) = \sum_{l=0}^{L-1} e_{ESE}(x_k^{\text{Re}}(j))_l. \quad (17b)$$

Comments:

- We obtain (14a)–(14d) using (12) and obtain (16a) as follows (based on (8) and (13)),

$$\text{Re}(\overline{h_{k,l}} \zeta_{k,l}(j)) = h_{k,l}^{\text{Re}} r^{\text{Re}}(j+l) + h_{k,l}^{\text{Im}} r^{\text{Im}}(j+l) - |h_{k,l}|^2 x_k^{\text{Re}}(j). \quad (18)$$

- It can be verified that $\Psi(j)$ in (15) is the covariance of $r^{\text{Re}}(j)$ and $r^{\text{Im}}(j)$. It is introduced for cost saving since it is shared by all users, costing L multiplications and $L/2$ additions per coded bit per user. (Recall that there are two coded bits in a chip, one in each dimension.)

- For the derivation of (16b), see the Appendix.
- A similar procedure can be used to estimate $x_k^{\text{Im}}(j)$ based on $\{\text{Im}(\overline{h_{k,l}}r(j+l)), l=0, \dots, L-1\}$.
- If the cost related to $\Psi(j)$ is ignored, the complexity of Algorithm 3 per coded bit per user is approximately two times of that of Algorithm 2. It slightly increases by several additions and multiplications considering $\Psi(j)$, but is still $O(L)$.

E. The ESE Function for Channels with Multiple Receive Antennas

The above principles can be easily generalized to channels with multiple receive antennas. The signals from each receive antenna can be treated as those from a set of independent paths. The LLRC technique discussed in Section II.C can be directly applied.

F. The DEC Function

The DEC in Fig. 1 carry out APP decoding using the output of the ESE as the input. With BPSK signaling, their output is the extrinsic LLRs $\{e_{DEC}(x_k(j))\}$ of $\{x_k(j)\}$ defined in (1), which are used to generate the following statistics

$$E(x_k(j)) = \tanh(e_{DEC}(x_k(j))/2), \quad (19a)$$

$$\text{Var}(x_k(j)) = 1 - (E(x_k(j)))^2. \quad (19b)$$

(With QPSK signaling, the DEC outputs are the extrinsic LLRs for $\{x_k^{\text{Re}}(j)\}$ and $\{x_k^{\text{Im}}(j)\}$.) As discussed above, $\{E(x_k(j))\}$ and $\{\text{Var}(x_k(j))\}$ will be used in the ESE to update the interference mean and variance in the next iteration. Initially, we set $E(x_k(j)) = 0$ and $\text{Var}(x_k(j)) = 1$ for $\forall k, j$.

APP decoding is a standard operation [1] and so we will not discuss it in detail. We will only consider a special case of C in Fig. 1 that is formed by serially concatenating a sub-code C_{FEC} (the same for every user) and a length- S repetition code C_{REP} . This scheme is not optimized from performance point of view, as the repetition code is actually a very ‘‘poor’’ code. However, this structure does have the advantage of flexibility regarding the rate.

The input data sequence of each user is first encoded by C_{FEC} , generating $\{b_k(i), i = 1, 2, \dots\}$. Then each $b_k(i)$ is repeated S times by C_{REP} , producing $\{c_k(j)\}$. For simplicity, we focus on those replicas related to $b_k(1)$, i.e., $\{c_k(j), j = 1, 2, \dots, S\}$. The treatment for replicas of $b_k(i)$ with i

> 1 is similar. The DEC for C carries out the following operations. For simplicity, we assume BPSK modulation.

- (i) Obtain the estimate of each $b_k(i)$ based on $\{e_{ESE}(x_k(j))\}$ from the ESE. We assume that $\{e_{ESE}(x_k(j)), \forall j\}$ are un-correlated (which is approximately true due to interleaving). From Fig. 1, we have $c_k(j) = x_k(\pi_k(j))$. Then the *a posteriori* LLR for $b_k(1)$ can be computed from $\{e_{ESE}(x_k(j))\}$ as [17]

$$L(b_k(1)) = \sum_{j=1}^S \log \left(\frac{\Pr(x_k(\pi_k(j)) = +1 | r(\pi_k(j)))}{\Pr(x_k(\pi_k(j)) = -1 | r(\pi_k(j)))} \right) = \sum_{j=1}^S e_{ESE}(x_k(\pi_k(j))). \quad (20)$$

- (ii) Perform standard APP decoding for C_{FEC} using $\{L(b_k(i))\}$ as the input, and generate the *a posteriori* LLRs $\{L_{APP}(b_k(i))\}$ for $\{b_k(i)\}$.
- (iii) Recall that $c_k(j) = b_k(1)$ for $j = 1, \dots, S$. We compute [17]

$$e_{DEC}(x_k(\pi_k(j))) = e_{DEC}(c_k(j)) = L_{APP}(b_k(1)) - e_{ESE}(x_k(\pi_k(j))), \quad j = 1, \dots, S. \quad (21a)$$

The subtraction above ensures that $e_{DEC}(x_k(\pi_k(j)))$ is extrinsic [1].

Alternatively, we can use an approximation of (21a),

$$e_{DEC}(x_k(\pi_k(j))) \approx L_{APP}(b_k(1)), \quad j = 1, \dots, S. \quad (21b)$$

In this way, all the replicas of $b_k(i)$ have the same feedback from the DEC, so the memory usage can be greatly reduced (since we only need to store $\{L_{APP}(b_k(i))\}$ instead of $\{e_{DEC}(x_k(j))\}$). Eqn. (21b) may lead to certain performance loss compared with (21a). See Fig. 3(a) in Section IV below.

G. The Cost of the Overall Receiver

The DEC cost of a cascade C_{FEC}/C_{REP} structure studied in Section II.F is dominated by the APP decoding cost for C_{FEC} , as the additional cost involved in (20) and (21) are usually marginal. In particular, suppose that a turbo type code is used as C_{FEC} . Then even a single-user detector would involve iterative processing with APP decoding. In this case, the extra cost for the multi-user detector described above is mainly related to the ESE, which, as we have seen, is very modest. The overall complexity of the multiuser detector can be roughly comparable to that of a single-user one. (The exact ratio depends on the cost ratio between the ESE and APP decoding.)

III. PERFORMANCE ANALYSIS

The performance analysis for a conventional CDMA multi-user detection scheme requires the knowledge of the correlation characteristics among signature sequences. It can be a quite complicated issue and sophisticated large random matrix theory has been used in the past to tackle the problem [9]-[10], [24].

IDMA does not involve signature sequences, which greatly simplifies the problem. In the following, we will derive a simple and efficient performance assessment technique. The method is semi-analytical since some of the functions involved (related to the FEC codes) are pre-calculated by simulation (similar to [14][15]). We will only discuss Algorithms 1 and 3, as Algorithm 2 is a special case of Algorithm 3.

A. Performance Assessment for Algorithm 1

Approximate $\text{Var}(\zeta_k(j))$ in (5d) by its sample mean

$$\text{Var}(\zeta_k(j)) \approx V_{\zeta_k} \equiv \sum_{k' \neq k} |h_{k'}|^2 V_{x_{k'}} + \sigma^2 \quad (22a)$$

where

$$V_{x_k} \equiv \frac{1}{J} \times \sum_{j=1}^J \text{Var}(x_k(j)) . \quad (22b)$$

(Notes: $\text{Var}(x_k(j))$ is the variance of a particular $x_k(j)$ obtained from a feedback $e_{DEC}(x_k(j))$ using (19b). V_{x_k} and V_{ζ_k} are averages of $\{\text{Var}(x_k(j)), \forall j\}$ and $\{\text{Var}(\zeta_k(j)), \forall j\}$ respectively, which can be different for different k due to the unequal fading coefficients for different users.)

Substituting (22) into (6), we have

$$e_{ESE}(x_k(j)) = \frac{2h_k}{V_{\zeta_k}} (h_k x_k(j) + \zeta_k(j) - \text{E}(\zeta_k(j))) . \quad (23)$$

In our study, we observed that (23) leads to slightly poorer performance compared with (6), since $\text{Var}(\zeta_k(j))$ carries more information about $\zeta_k(j)$ (for a particular j) than V_{ζ_k} . Thus, replacing (6) by (23) is a pessimistic approximation. However, this replacement greatly simplifies the analysis issue. Similar techniques have been used in [9][24] for CDMA receiver analysis.

In (23), $h_k x_k(j)$ and $\zeta_k(j) - \mathbb{E}(\zeta_k(j))$ represent signal and distortion components, respectively. Since $x_k(j) = \pm 1$, signal power $\mathbb{E}(|h_k x_k(j)|^2) = |h_k|^2$. We approximate the average noise power after soft cancellation (for a fixed k) by its sample mean,

$$\mathbb{E}(|\zeta_k(j) - \mathbb{E}(\zeta_k(j))|^2) \approx V_{\zeta_k}. \quad (24)$$

The coefficient $2h_k/V_{\zeta_k}$ in (23) is a constant factor that does not affect the SNR. The average SNR of $e_{ESE}(x_k(j))$ over j , denoted by snr_k , is thus given by

$$snr_k = \frac{\mathbb{E}(|h_k x_k(j)|^2)}{V_{\zeta_k}} = \frac{|h_k|^2}{\sum_{k'} |h_{k'}|^2 V_{x_{k'}} - |h_k|^2 V_{x_k} + \sigma^2}. \quad (25)$$

We assume that $\{e_{ESE}(x_k(j)), \forall j\}$ can be approximately treated as LLRs of $\{x_k(j), \forall j\}$ generated from the observations of an AWGN channel with SNR equal to snr_k . This implies that the distortion components among $\{e_{ESE}(x_k(j)), \forall j\}$ are un-correlated, which is approximately true when the frame length $J \rightarrow \infty$. Recall that $\text{Var}(x_k(j))$ in (19b) is calculated based on $e_{DEC}(x_k(j))$, so V_{x_k} in (22b) is a function of snr_k ,

$$V_{x_k} = f(sn�_k). \quad (26)$$

In general, there is no closed form expression for $f(\cdot)$, but it can be easily obtained by the Monte Carlo method. This only involves simulating a single-user APP decoder for C in an AWGN channel with specified SNRs. We assume that all users use the same FEC code, so $f(\cdot)$ is the same for all users. Similarly, we can define the bit-error-rate (BER) performance for the k th DEC as a function of snr_k ,

$$\text{BER} = g(sn�_k) \quad (27)$$

which can also be obtained by simulation. Combining (25) and (26), we have

$$snr_{k_new} = \frac{|h_k|^2}{\sum_{k'} |h_{k'}|^2 f(sn�_{k'_old}) - |h_k|^2 f(sn�_{k_old}) + \sigma^2}, \quad (28)$$

where snr_{k_new} and snr_{k_old} are, respectively, snr_k values after and before one iteration. At the start, we initialize $f(sn�_{k_old}) = 1$ for all k , implying no feedback from the DECs. Repeating (28), we can track the SNR evolution for the iterative process. During the final iteration, we can estimate the BER performance of all users using (27): $\text{BER} = g(sn�_{k_final})$, $k=1, 2, \dots$

B. Performance Assessment for Algorithm 3

We now consider Algorithm 3. With QPSK signaling, each $x_k(j)$ contains two coded bits in the real and imaginary parts respectively, and V_{x_k} in (22b) is modified as

$$V_{x_k} \equiv \frac{1}{2J} \times \sum_{j=1}^J (\text{Var}(x_k^{\text{Re}}(j)) + \text{Var}(x_k^{\text{Im}}(j))) . \quad (29)$$

Similar to (22a), we adopt the following approximation

$$\text{Var}(x_k^{\text{Re}}(j)) \approx \text{Var}(x_k^{\text{Im}}(j)) \approx V_{x_k} . \quad (30)$$

Substitute (30) into (14) ~ (16). Then (17a) can be modified as

$$e_{ESE}(x_k^{\text{Re}}(j))_l = 2 \frac{|h_{k,l}|^2}{V_{\zeta_{k,l}}} \cdot \left(|h_{k,l}|^2 x_k^{\text{Re}}(j) + \text{Re}(\overline{h_{k,l}} \zeta_{k,l}(j)) - \text{E}(\text{Re}(\overline{h_{k,l}} \zeta_{k,l}(j))) \right) \quad (31)$$

where (after replacing $\text{Var}(x_k^{\text{Re}}(j))$ and $\text{Var}(x_k^{\text{Im}}(j))$ by V_{x_k} in (14c) - (16b)),

$$V_{\zeta_{k,l}} = |h_{k,l}|^2 \sum_{k',l'} |h_{k',l'}|^2 V_{x_{k'}} - |h_{k,l}|^4 V_{x_k} + |h_{k,l}|^2 \sigma^2 . \quad (32)$$

Similar to (24), we approximate the average noise power after soft cancellation by $V_{\zeta_{k,l}}$, i.e.,

$$\text{E} \left(\left| \text{Re}(\overline{h_{k,l}} \zeta_{k,l}(j)) - \text{E}(\text{Re}(\overline{h_{k,l}} \zeta_{k,l}(j))) \right|^2 \right) \approx V_{\zeta_{k,l}} . \quad (33)$$

Then the average SNR for $e_{ESE}(x_k^{\text{Re}}(j))_l$, denoted by $snr_{k,l}$, is given by

$$snr_{k,l} = \frac{\text{E} \left(\left(|h_{k,l}|^2 x_k^{\text{Re}}(j) \right)^2 \right)}{V_{\zeta_{k,l}}} = \frac{|h_{k,l}|^2}{\sum_{k',l'} |h_{k',l'}|^2 V_{x_{k'}} - |h_{k,l}|^2 V_{x_k} + \sigma^2} . \quad (34)$$

Substituting (31) into (17b), we have

$$e_{ESE}(x_k^{\text{Re}}(j)) = 2 \sum_l \frac{|h_{k,l}|^2}{V_{\zeta_{k,l}}} \cdot \left(|h_{k,l}|^2 x_k^{\text{Re}}(j) + \text{Re}(\overline{h_{k,l}} \zeta_{k,l}(j)) - \text{E}(\text{Re}(\overline{h_{k,l}} \zeta_{k,l}(j))) \right) . \quad (35a)$$

We view $|h_{k,l}|^2 x_k^{\text{Re}}(j)$ and $\text{Re}(\overline{h_{k,l}} \zeta_{k,l}(j)) - \text{E}(\text{Re}(\overline{h_{k,l}} \zeta_{k,l}(j)))$ in (35a) as signal and distortion components, respectively. Their SNR ratio is given by $|h_{k,l}|^2 / V_{\zeta_{k,l}}$. Thus, besides a scaling

factor of 2, (35a) can be regarded as a maximum ratio combining (MRC) of L independent distorted signals $\left\{ |h_{k,l}|^2 x_k^{\text{Re}}(j) + \text{Re}(\overline{h_{k,l}} \zeta_{k,l}(j)) - \text{E}(\text{Re}(\overline{h_{k,l}} \zeta_{k,l}(j))), l = 0, \dots, L-1 \right\}$. Following the

discussion in [25] on MRC, the average SNR for $e_{ESE}(x_k^{\text{Re}}(j))$, denoted by snr_k , is simply

$$snr_k = \sum_l snr_{k,l} . \quad (35b)$$

Similarly, it can be verified that the average SNR of $e_{ESE}(x_k^{\text{Im}}(j))$ over j has the same expression as (35). Combining (35) and (26), we have (for either $e_{ESE}(x_k^{\text{Re}}(j))$ or $e_{ESE}(x_k^{\text{Im}}(j))$)

$$snr_{k_new} = \sum_l \frac{|h_{k,l}|^2}{\sum_{k',l'} |h_{k',l'}|^2 f(sn r_{k'_old}) - |h_{k,l}|^2 f(sn r_{k_old}) + \sigma^2} . \quad (36)$$

It is interesting to note the similarity between (28) and (36).

IV. NUMERICAL RESULTS

Let N_{info} be the number of information bits in a frame, K the number of simultaneous users in the system, L the tap number of an ISI channel, N_r the number of receive antennas, l the iteration number, R_C the rate of each user, and $K \times R_C$ the system throughput that is a measurement of the overall bandwidth efficiency. QPSK signaling is always assumed.

First we consider constructing C using a common rate-1/2 $(23, 35)_8$ convolutional code followed by (i.e., in serial concatenation with) a length-8 repetition code ($R_C = 1/2 \times 1/8 = 1/16$). The repetition coding can be viewed as a kind of spreading, except that all of the users use the same sequence. The resultant codeword is then multiplied by a mask sequence with alternative signs, i.e., $[+1, -1, +1, -1, \dots]$, to balance the numbers of $+1$ and -1 . Two independent chip interleavers are employed by each user to produce the in-phase and quadrature parts of the transmitted sequence. The purpose of the masking operation is to maximize the randomness among the transmitted sequences of different users.

Fig. 2 shows the curves of $f(\cdot)$ in (26) and $g(\cdot)$ in (27) obtained by Monte Carlo simulations for the concatenation of the convolutional code and the repetition code in an AWGN channel.

Fig. 3 compares the evolution and simulation results of the above system in an AWGN channel. The single-user performance is also included for reference. We compare three methods, namely, the semi-analytical approach discussed in Section III and the simulation methods using either (21a) or (21b) in DECs. The simulation results (using (21a) in DECs) and evolution results are quite close for different K (Fig. 3(a)) and for different iteration numbers (Fig. 3(b)), which confirms the viability of the semi-analytical method.

For the low-cost option (21b), its performance is close to that of (21a) when K is not very large. However, when $K \geq 24$, the performance deterioration due to the use of (21b) becomes noticeable.

Fig. 4 shows the performance of Algorithm 3 applied to the above system in quasi-static Rayleigh fading multipath channels with different channel tap numbers and receive antenna numbers. The corresponding single-user performance is also included for reference. It is

observed that the system can achieve $K \times R_C = 3$ bits/chip for $K = 48$ using one receive antenna and $K \times R_C = 6$ bits/chip for $K = 96$ using two receive antennas with performance close to the single-user performance at $\text{BER} = 10^{-4}$. Such throughputs are rather high, recalling that with TDMA we may require a 128-QAM trellis coded modulation scheme to achieve similar throughput and performance.

Next we consider using a more sophisticated low-rate code to improve power efficiency that is closely related to spectral efficiency. With higher power efficiency, the transmission power of each user can be reduced. Since the performance of cellular systems is mainly limited by the interference among users, lower transmission power from each user leads to reduced interference. Consequently a larger number of simultaneous users can be supported in a cellular environment [26]. We adopt a turbo-Hadamard code [27] constructed by concatenating 3 convolutional-Hadamard codes in parallel, each generated from a length-32 Hadamard code and a convolutional code with polynomial $G(x) = 1/(1+x)$. The information bits in all component codes except one are punctured. A random puncturing operation on parity bits is also adopted to make $R_C = 1/16$.

Fig. 5 illustrates the performance of an IDMA system based on the turbo-Hadamard code (Scheme I) in AWGN channels. From Fig. 5, performance of $\text{BER} = 10^{-5}$ is observed at $E_b/N_0 \approx 1.4$ dB with $K = 16$, which corresponds to $K \times R_C = 1$ bit/chip. This is only about 1.4 dB away from the corresponding Shannon limit, which is $E_b/N_0 = 0$ dB for a throughput of 1 bit/chip, the same as that for a single-user AWGN channel [12].

For comparison, we have also included in Fig. 5 the performance of an IDMA system based on a standard turbo code (Scheme II), in which C is constructed using a rate-1/3 $(1, 35/23)_8$ turbo code followed by a length-6 repetition code. Puncturing is then applied to make $R_C = 1/16$. The advantage of using a low-rate code is clearly seen from Fig. 5. With $K = 16$, Scheme I demonstrates about 1dB performance advantage over Scheme II, due to the higher coding gain offered by the turbo-Hadamard code. The decoding costs of Schemes I and II are quite similar.

V. CONCLUSIONS

We have presented several simple detection algorithms for various channels and developed a semi-analytical technique to track the SNR evolution for these algorithms, based on which the performance of IDMA systems can be accurately predicted. The benefits of the IDMA scheme are substantial as seen from Figs. 3 to 5. These include low-cost MUD for systems with large numbers of users, robustness and diversity in multipath environments, very high spectral efficiency and near limit performance.

In conclusion, we have explained the feasibility and advantages of the interleaver-based multiple access scheme together with an accurate and effective performance prediction technique. We expect that the basic principles can be extended to other applications, such as space-time codes [18] and ultra wideband (UWB) systems [28].

APPENDIX. THE DERIVATION OF EQN. (16b)

Based on (13), the left hand side (LHS) of (16b) can be divided into two parts as

$$\text{Var}\left(\text{Re}\left(\overline{h_{k,l}}\zeta_{k,l}(j)\right)\right) = \text{Var}\left(\text{Re}\left(\overline{h_{k,l}}r(j+l)\right)\right) - |h_{k,l}|^4 \text{Var}(x_k^{\text{Re}}(j)). \quad (\text{A.1})$$

From (12),

$$\begin{aligned} \text{Re}\left(\overline{h_{k,l}}r(j+l)\right) &= h_{k,l}^{\text{Re}}r^{\text{Re}}(j+l) + h_{k,l}^{\text{Im}}r^{\text{Im}}(j+l) \\ &= h_{k,l}^{\text{Re}}\left(\sum_{k',l'}\left(h_{k',l'}^{\text{Re}}x_{k'}^{\text{Re}}(j+l-l') - h_{k',l'}^{\text{Im}}x_{k'}^{\text{Im}}(j+l-l')\right)\right) \\ &\quad + h_{k,l}^{\text{Im}}\left(\sum_{k',l'}\left(h_{k',l'}^{\text{Im}}x_{k'}^{\text{Re}}(j+l-l') + h_{k',l'}^{\text{Re}}x_{k'}^{\text{Im}}(j+l-l')\right)\right) + \text{Re}\left(\overline{h_{k,l}}n(j+l)\right) \\ &= \sum_{k',l'}\left(h_{k,l}^{\text{Re}}h_{k',l'}^{\text{Re}} + h_{k,l}^{\text{Im}}h_{k',l'}^{\text{Im}}\right)x_{k'}^{\text{Re}}(j+l-l') \\ &\quad + \sum_{k',l'}\left(-h_{k,l}^{\text{Re}}h_{k',l'}^{\text{Im}} + h_{k,l}^{\text{Im}}h_{k',l'}^{\text{Re}}\right)x_{k'}^{\text{Im}}(j+l-l') + \text{Re}\left(\overline{h_{k,l}}n(j+l)\right). \end{aligned} \quad (\text{A.2})$$

$$\begin{aligned} &\text{Var}\left(\text{Re}\left(\overline{h_{k,l}}r(j+l)\right)\right) \\ &= \sum_{k',l'}\left(h_{k,l}^{\text{Re}}h_{k',l'}^{\text{Re}} + h_{k,l}^{\text{Im}}h_{k',l'}^{\text{Im}}\right)^2 \text{Var}(x_{k'}^{\text{Re}}(j+l-l')) \\ &\quad + \sum_{k',l'}\left(-h_{k,l}^{\text{Re}}h_{k',l'}^{\text{Im}} + h_{k,l}^{\text{Im}}h_{k',l'}^{\text{Re}}\right)^2 \text{Var}(x_{k'}^{\text{Im}}(j+l-l')) + |h_{k,l}|^2 \sigma^2 \\ &= \left(h_{k,l}^{\text{Re}}\right)^2 \sum_{k',l'}\left(\left(h_{k',l'}^{\text{Re}}\right)^2 \text{Var}(x_{k'}^{\text{Re}}(j+l-l')) + \left(h_{k',l'}^{\text{Im}}\right)^2 \text{Var}(x_{k'}^{\text{Im}}(j+l-l'))\right) + \left(h_{k,l}^{\text{Re}}\right)^2 \sigma^2 \\ &\quad + \left(h_{k,l}^{\text{Im}}\right)^2 \sum_{k',l'}\left(\left(h_{k',l'}^{\text{Im}}\right)^2 \text{Var}(x_{k'}^{\text{Re}}(j+l-l')) + \left(h_{k',l'}^{\text{Re}}\right)^2 \text{Var}(x_{k'}^{\text{Im}}(j+l-l'))\right) + \left(h_{k,l}^{\text{Im}}\right)^2 \sigma^2 \\ &\quad + 2h_{k,l}^{\text{Re}}h_{k,l}^{\text{Im}} \sum_{k',l'} h_{k',l'}^{\text{Re}}h_{k',l'}^{\text{Im}} \left(\text{Var}(x_{k'}^{\text{Re}}(j+l-l')) - \text{Var}(x_{k'}^{\text{Im}}(j+l-l'))\right) \end{aligned} \quad (\text{A.3})$$

Substituting (14c), (14d) and (15) into (A.3) gives,

$$\text{Var}\left(\text{Re}\left(\overline{h_{k,l}}r(j+l)\right)\right) = \left(h_{k,l}^{\text{Re}}\right)^2 \text{Var}\left(r^{\text{Re}}(j+l)\right) + \left(h_{k,l}^{\text{Im}}\right)^2 \text{Var}\left(r^{\text{Im}}(j+l)\right) + 2h_{k,l}^{\text{Re}}h_{k,l}^{\text{Im}}\Psi(j+l) \quad (\text{A.4})$$

Finally, (16b) results from substituting (A.4) into (A.1).

REFERENCES

- [1] C. Berrou and A. Glavieux, "Near Shannon limit error correcting coding and decoding: Turbo-codes," *IEEE Trans. Commun.*, vol. 44, pp. 1261–1271, Oct. 1996.
- [2] M. Moher and P. Guinand, "An iterative algorithm for asynchronous coded multi-user detection," *IEEE Commun. Lett.*, vol. 2, pp. 229–231, Aug. 1998.
- [3] M. C. Reed, C. B. Schlegel, P. D. Alexander, and J. A. Asenstorfer, "Iterative multi-user detection for CDMA with FEC: Near-single-user performance," *IEEE Trans. Commun.*, vol. 46, pp. 1693–1699, Dec. 1998.
- [4] X. Wang and H. V. Poor, "Iterative (turbo) soft interference cancellation and decoding for coded CDMA," *IEEE Trans. Commun.*, vol. 47, pp. 1046–1061, July 1999.
- [5] Z. Shi and C. Schlegel, "Joint iterative decoding of serially concatenated error control coded CDMA," *IEEE J. Select. Areas Commun.*, vol. 19, pp. 1646–1653, Aug. 2001.
- [6] A. AlRustamani, A. D. Damnjanovic, and B. R. Vojcic, "Turbo greedy multi-user detection," *IEEE J. Select. Areas Commun.*, vol. 19, pp. 1638–1645, Aug. 2001.
- [7] A. AlRustamani and B. R. Vojcic, "A new approach to greedy multi-user detection," *IEEE Trans. Commun.*, vol. 50, pp. 1326–1336, Aug. 2002.
- [8] M. C. Reed and P. D. Alexander, "Iterative multi-user detection using antenna arrays and FEC on multipath channels," *IEEE J. Select. Areas Commun.*, vol. 17, pp. 2082–2089, Dec. 1999.
- [9] J. Boutros and G. Carie, "Iterative multi-user joint decoding: Unified framework and asymptotic analysis," *IEEE Trans. Inform. Theory*, vol. 48, pp. 1772–1793, July 2002.
- [10] M. L. Honig, R. Ratasuk, "Large-system performance of iterative multiuser decision-feedback detection," *IEEE Trans. Commun.*, vol. 51, pp. 1368–1377, Aug. 2003.
- [11] A. J. Viterbi, "Very low rate convolutional codes for maximum theoretical performance of spread spectrum multiple-access channels," *IEEE J. Select. Areas Commun.*, vol. 8, pp. 641–649, Aug. 1990.
- [12] S. Verdú and S. Shamai, "Spectral efficiency of CDMA with random spreading," *IEEE Trans. Inform. Theory*, vol. 45, pp. 622–640, Mar. 1999.
- [13] J. Y. N. Hui, "Throughout analysis for code division multiple accessing of the spread spectrum channel," *IEEE J. Select. Areas Commun.*, vol. 2, pp. 482–486, July 1984.
- [14] F. N. Brannstrom, T. M. Aulin, and L. K. Rasmussen, "Iterative decoders for trellis code multiple-access," *IEEE Trans. on Commun.*, vol. 50, pp. 1478–1485, Sept. 2002.
- [15] S. Brück, U. Sorger, S. Gligorevic, and N. Stolte, "Interleaving for outer convolutional codes in DS-CDMA Systems," *IEEE Trans. Commun.*, vol. 48, pp. 1100–1107, July 2000.

- [16] A. Tarable, G. Montorsi, and S. Benedetto, "Analysis and design of interleavers for CDMA systems," *IEEE Commun. Lett.*, vol. 5, pp. 420–422, Oct. 2001.
- [17] R. H. Mahadevappa and J. G. Proakis, "Mitigating multiple access interference and intersymbol Interference in uncoded CDMA Systems with chip-level interleaving," *IEEE Trans. Wireless Commun.*, vol. 1, pp. 781–792, Oct. 2002.
- [18] Li Ping, L. Liu, K. Y. Wu, and W. K. Leung, "A unified approach to multi-user detection and space-time coding with low complexity and nearly optimal performance," in *Proc. 40th Allerton Conference*, Allerton House, USA, Oct. 2002, pp. 170–179 (www.ee.cityu.edu.hk/~liping/research).
- [19] L. Liu, W. K. Leung, and Li Ping, "Simple chip-by-chip multi-user detection for CDMA systems," in *Proc. IEEE VTC-Spring*, Jeju, Korea, Apr. 2003, pp. 2157–2161.
- [20] Li Ping, L. Liu, K. Y. Wu, and W. K. Leung, "Approaching the capacity of multiple access channels using interleaved low-rate codes," *IEEE Commun. Letters*, vol. 8, pp. 4-6, Jan, 2004.
- [21] T. Richardson and R. Urbanke, "The capacity of low density parity check codes under message passing decoding," *IEEE Trans. Inform. Theory*, vol. 47, pp. 599–618, Feb. 2001.
- [22] S. ten Brink, "Convergence behavior of iteratively decoded parallel concatenated codes," *IEEE Trans. Commun.* vol. 49, pp. 1727–1737, Oct. 2001.
- [23] D. Divsalar, S. Dolinar, and F. Pollara, "Iterative turbo decoder analysis based on density evolution," *IEEE J. Select. Areas Commun.*, vol. 19, pp. 891–907, May 2001.
- [24] J. Zhang, E. K. P. Chong and D. N. C. Tse "Output MAI distributions of linear MMSE multiuser receivers in DS-CDMA systems," *IEEE Trans. on Inform. Theory*, vol. 47, pp. 1128-1144, Mar. 2001.
- [25] T. S. Rappaport, *Wireless Communications Principle and Practice*. Prentice-Hall. 1996.
- [26] K. S. Gilhousen, I. M. Jacobs, R. Padovani, A. J. Viterbi, L. A. Weaver, and C. E. Wheatly, "On the capacity of a cellular CDMA system," *IEEE Trans. Vehicular Technology*, vol. 40, pp. 303–312, May 1991.
- [27] Li Ping, W. K. Leung, and K. Y. Wu, "Low-rate turbo-Hadamard codes," *IEEE Trans. Inform. Theory*, vol. 49, pp. 3213–3224, Dec. 2003.
- [28] E. Fishler and H. V. Poor, "On the tradeoff between two types of processing gain," in *Proc. 40th Allerton Conference*, Allerton House, USA, Oct. 2002, pp. 1178–1187.

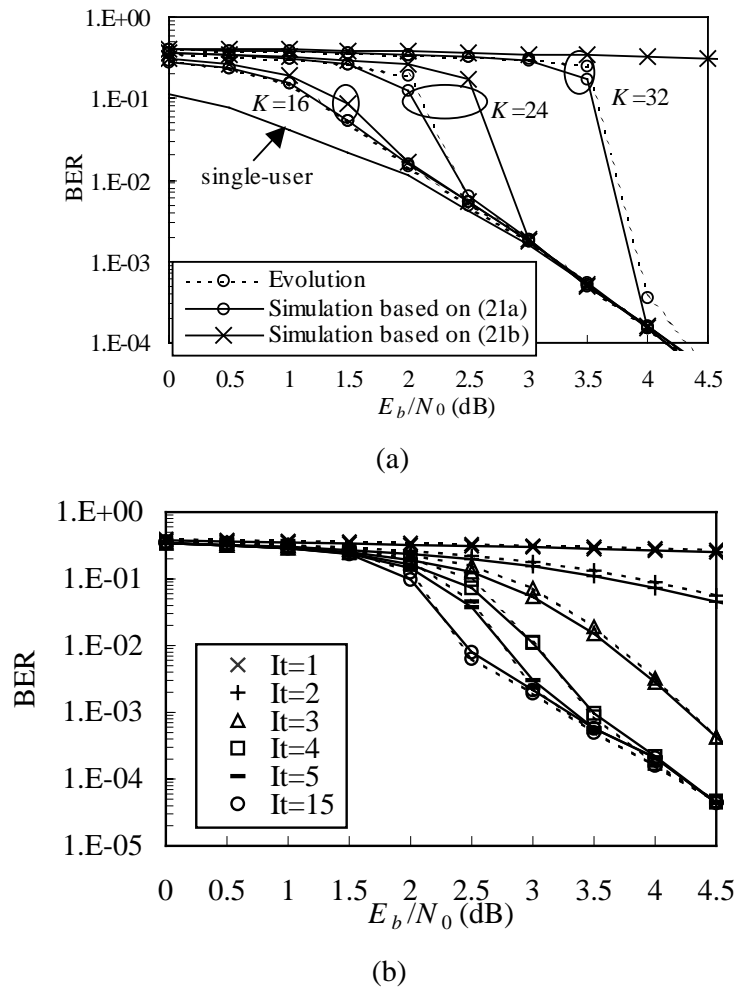


Figure 3. Comparison between the evolution and simulation results of a convolutionally coded IDMA system in AWGN channels. $N_{\text{info}} = 1024$ and $N_r = 1$. (a) For different numbers of simultaneous users K and $I_t = 15$. (b) For different iteration numbers I_t and $K = 24$. Dashed lines represent evolution results and solid lines represent simulation results (using (21a) in DEC's).

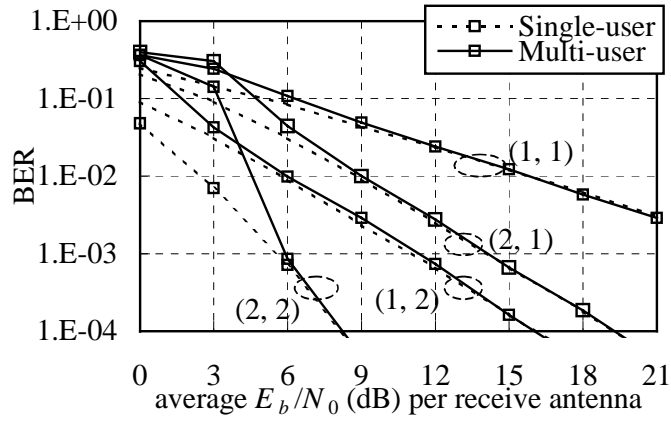


Figure 4. Performance of a convolutionally coded IDMA system in quasi-static multipath Rayleigh fading channels. The (L, N_r) pair is marked in the figure. $K = 48$ for one receive antenna and $K = 96$ for two receive antennas. $N_{\text{info}} = 128$ and $It = 10$.

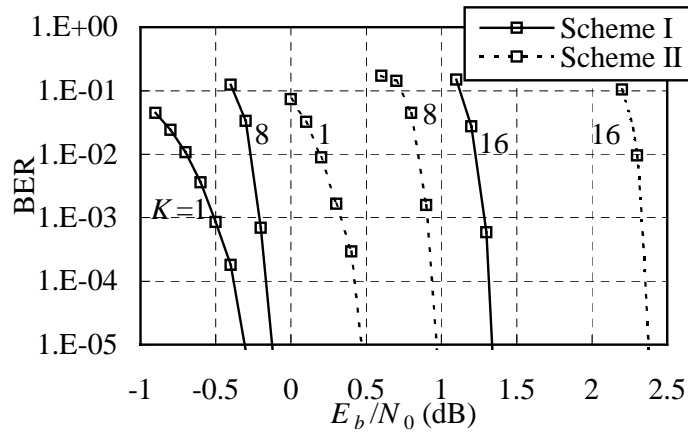


Figure 5. Performance of IDMA systems based on the turbo-Hadamard code [27] and turbo code over AWGN channels. $N_r = 1$, $It = 30$, $N_{\text{info}} = 4095$ for Scheme I and $N_{\text{info}} = 4096$ for Scheme II.